Mutagenic Product Formation Due to Reaction of Guanine Radical Cation with Nitrogen Dioxide

ARTICLE *in* THE JOURNAL OF PHYSICAL CHEMISTRY B · APRIL 2009

Impact Factor: 3.3 · DOI: 10.1021/jp805942y · Source: PubMed

2 AUTHORS, INCLUDING:

P.C. Mishra
Banaras Hindu University
156 PUBLICATIONS **1,804** CITATIONS

Mutagenic Product Formation Due to Reaction of Guanine Radical Cation with Nitrogen Dioxide

Neha Agnihotri and P. C. Mishra*

Department of Physics, Banaras Hindu University, Varanasi - 221 005, India

Received: July 6, 2008; Revised Manuscript Received: December 3, 2008

The reaction between nitrogen dioxide ($NO_2^{\cdot}$) and guanine radical cation ($G^{\cdot+}$) yielding the mutagenic product 8-nitroguanine radical cation (8-nitro$G^{\cdot+}$) was studied in the presence of one or two water molecules. All the relevant extrema on the potential energy surface were located by fully optimizing the geometries of the reactant, intermediate, and product complexes as well as transition states at the B3LYP/6-31G**, B3PW91/6-31G**, B3LYP/AUG-cc-pVDZ, and B3PW91/AUG-cc-pVDZ levels of density functional theory in gas phase. Zero point energy-corrected total energies and the corresponding Gibbs free energies at 298.15 K were obtained at the B3LYP/AUG-cc-pVDZ and B3PW91/AUG-cc-pVDZ levels of theory. Single point energy calculations were performed for all the optimized geometries at the MP2/AUG-cc-pVDZ level of theory in gas phase. Solvent effect of aqueous media was treated by performing single point energy calculations at the B3LYP/AUG-cc-pVDZ, B3PW91/AUG-cc-pVDZ, and MP2/AUG-cc-pVDZ levels of theory employing the polarizable continuum model. The solvent effect of bulk water as well as that due to specific water molecules were found to play very important roles in lowering down many barrier energies appreciably. It is found that 8-nitro$G^{\cdot+}$ complexed with water molecules would be formed due to the reaction of $G^{\cdot+}$ with $NO_2^{\cdot}$ in aqueous media. The possible biological significance of the results obtained has been examined by studying binding energies of several normal and abnormal base pairs.

1. Introduction

Reactive oxygen species (ROS) and reactive nitrogen oxide species (RNOS) play an important role in aging, mutation, and cancer.[1] The most common ROS and RNOS present in the biological enviroment are superoxide radical anion ($O_2^{\cdot-}$), hydroxyl radical ($OH^{\cdot}$), peroxyl radical ($RO_2^{\cdot}$), alkoxyl radical ($RO^{\cdot}$), (R = alkyl group), HOCl, H_2O_2, H_2O_3, peroxynitrite ($ONOO^-$), $NO^{\cdot}$, $NO_2^{\cdot}$, and so forth.[1] Among the various ROS and RNOS, peroxynitrite is of great importance as it plays a major role in oxidation and nitration of biomolecules.[2−4] It can be formed due to reaction between nitric oxide radical ($NO^{\cdot}$) and superoxide radical anion ($O_2^{\cdot-}$) which are associated with inflammation of cells.[5,6] It can react with almost all biomolecules including DNA, proteins, and lipids under favorable conditions.[3,7−9] Reaction of peroxynitrite with guanine leads to the formation of 8-oxoguanine (8-oxoG) and 8-nitroguanine (8-nitroG).[10−12] 8-oxoG readily mispairs with adenine during DNA replication that causes GC to AT transversion mutation.[13] Repair mechanisms operate in biological media to remove this mispairing from DNA,[14−16] but it is not fully removed and leads to aging, mutation, and cancer.[17,18] Similarly, formation of 8-nitroG also initiates mutation, inflammation, and cancer.[19] Formation of radicals in the C-G base pair and its possible biological consequences, including the possible formation of 8-oxoG, have been studied by Bera and Schaefer.[20] It has been reported that guanine in DNA is preferentially oxidized by $Br_2^{\cdot-}$ to 8-oxoG that acts a trap for radiation-produced holes.[21] A theoretical study has indicated that mutagenically significant amounts of minor tautomeric forms of 8-oxoG would exist in aqueous media.[22] In previous studies,[23−29] the solvent effect of aqueous media on the properties of some biomolecules, particularly amino acids, for example, vibrational spectra and isomerization, was investigated using experimental as well as ab initio, density functional theoretic and molecular dynamics methods. These studies have demonstrated the importance of specific water molecules surrounding the solutes.[23−29]

It has been observed that CO_2 and bicarbonate strongly affect the rate constants and product yields of reactions of peroxynitrite with different biomolecules including DNA.[30−34] Reaction of peroxynitrite with CO_2 leads to the formation of nitrosoperoxycarbonate anion ($ONOOCO2^-$) which is highly reactive toward biomolecules.[34−42] This species dissociates into two components, that is, nitrogen dioxide radical ($NO_2^{\cdot}$) and carbonate radical anion ($CO_3^{\cdot-}$).[42,43] $NO_2^{\cdot}$ is recognized as a highly reactive free radical RNOS that produces serious consequences in biological media.[43] It can cause injury by oxidative reactions with proteins in tissues. In some cases, reaction of $NO_2^{\cdot}$ with biomolecules can also cause cell death.[44−46]

Among the four DNA bases, guanine is frequently attacked by ROS and RNOS.[1,12,44,45] Ground- and excited-state properties of guanine and 2′-deoxyguanosine have been studied extensively.[47,48] It is found that $NO_2^{\cdot}$ does not easily react with neutral guanine.[44] Instead, it reacts readily with neutral guanine radical G(-H)$^{\cdot}$ and guanine radical cation ($G^{\cdot+}$).[46] Formation of $G^{\cdot+}$ has been observed in pulse radiolysis experiments by oxidation of guanine without deprotonation.[49,50] It has been observed that electron holes created by one-electron oxidation of oligonucleotides in solution can migrate for long distances in DNA and are trapped at guanines as guanine has the lowest ionization potential among the bases.[51−55] A comparative study of reactivity of $NO_2^{\cdot}$ toward neutral guanine radical and guanine radical cation has been carried out by Liu et al.[46] at the B3LYP/6-31G** level of theory along with single point energy calcula-

* To whom correspondence should be addressed. E-mail: pcmishra_in@yahoo.com.

10.1021/jp805942y CCC: $40.75
Published on Web 02/17/2009

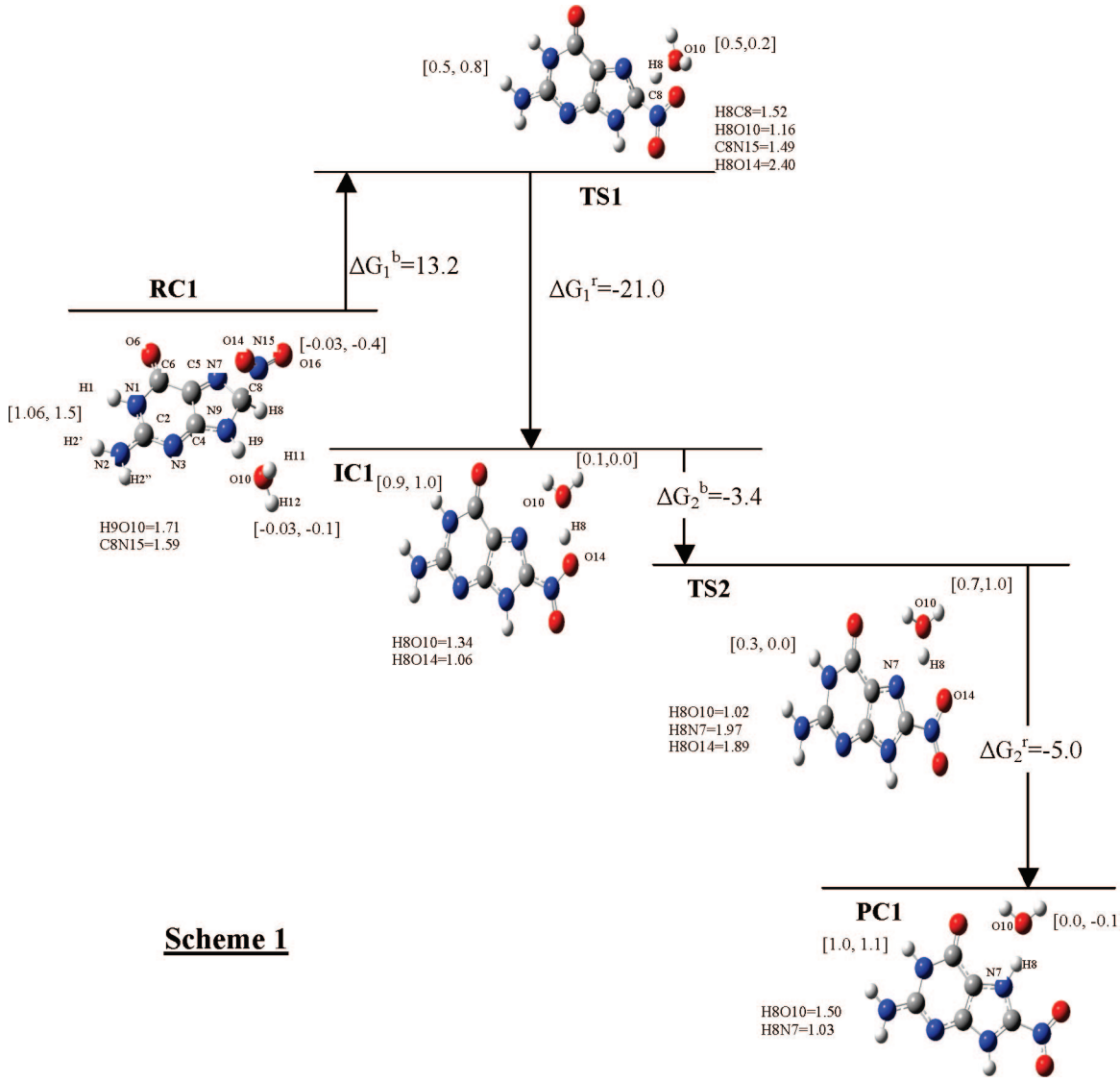

Figure 1. Reactant complex (RC1), intermediate complex (IC1), product complex (PC1), and transition states (TS1, TS2) involved in the reaction of $NO_2^{\cdot}$ at the C8 site of $G^{\cdot+}$ in the presence of a water molecule placed near the C8 atom of $G^{\cdot+}$. Gibbs free energy changes at 298.15 K (kcal/mol), CHelpG and Mulliken charges (first and second, respectively in the brackets) associated with different moieties obtained at the MP2/AUG-cc-pVDZ level of theory in aqueous media are given. Certain optimized interatomic distances (Å) are also given. The locations of different structures in terms of energy values are not to scale.

tions in gas phase at the B3LYP/6-311++G level and geometry optimization in aqueous media employing the Onsager model which treats the solvent effect approximately considering the solute as a dipole. It has been shown that the reaction of $NO_2^{\cdot}$ with guanine radical cation is much more favored than that with neutral guanine radical.[46] In this work,[46] some reaction steps between $NO_2^{\cdot}$ and guanine radical cation have also been worked out.[46] However, it is desirable that a detailed systematic study of the reaction of $NO_2^{\cdot}$ with guanine radical cation explaining the different possible reaction mechanisms in terms of reactant complexes, transition states, intermediate complexes and product complexes including the specific and bulk solvent effects of aqueous media be performed so that the favored reaction paths can be established. The results of such a study are presented here.

2. Computational Details

Geometries of all the reactant, intermediate, and product complexes as well as transition states involved in the reaction of $NO_2^{\cdot}$ with the guanine radical cation ($G^{\cdot+}$) in the presence of one or two water molecules were fully optimized in gas phase at the B3LYP/6-31G**, B3PW91/6-31G**, B3LYP/AUG-cc-pVDZ, and B3PW91/AUG-cc-pVDZ levels of density functional theory (DFT).[56,57] Geometry optimization calculations were also carried out at the BHandHLYP/AUG-cc-pVDZ level of theory in gas phase for one of the reaction schemes (Figure 1). Single point energy calculations at the MP2/AUG-cc-pVDZ level of theory in gas phase were carried out for all the geometries optimized at the B3LYP/AUG-cc-pVDZ level. Numbers of negative eigenvalues of the second derivative on the PES were tracked for locating total energy minima and transition states.[58] Minima had no negative eigenvalue (all real vibrational frequencies) while transition states had one negative eigenvalue (one imaginary vibrational frequency) each. Solvation in aqueous media was treated by single point energy calculations at the B3LYP/AUG-cc-pVDZ and MP2/AUG-cc-pVDZ levels of theory using the polarizable continuum model (PCM)[59,60] and employing the geometries optimized at the B3LYP/AUG-cc-pVDZ level in gas phase. Solvation in aqueous media was also treated by single point energy calculations at the B3PW91/AUG-

TABLE 1: ZPE-Corrected Barrier Energies (ΔE_i^b) and the Corresponding Gibbs Free Energy Changes (ΔG_i^b) ($i = 1, 2$) at 298.15 K (kcal/mol) Involved in the Reaction of $NO_2^{\cdot}$ with $G^{\cdot+}$ in the Presence of a Water Molecule Placed near the C8 Site of $G^{\cdot+}$, According to Figure 1

	gas phase						aqueous media		
barrier energies and corresponding Gibbs free energy changes	B3LYP/6-31G**	B3LYP/AUG-cc-pVDZ	B3PW91/6-31G**	B3PW91/AUG-cc-pVDZ	BH and HLYP/AUG-cc-pVDZ	MP2/AUG-cc-pVDZ	B3LYP/AUG-cc-pVDZ	B3PW91/AUG-cc-pVDZ	MP2/AUG-cc-pVDZ
ΔE_1^b	17.1	19.7	15.3	17.4	23.4	19.5	13.5	12.5	10.9
ΔG_1^b	19.6	22.1	17.5	19.7	25.7	21.8	15.8	14.8	13.2
ΔE_2^b	8.6	9.1	7.7[a]	8.6[a]	7.3	4.1	1.3	0.2	−3.8
ΔG_2^b	9.0	9.5	8.3[a]	9.0[a]	7.8	4.5	1.7	0.7	−3.4

[a] Obtained by single point energy calculations using the geometry optimized at the B3LYP/AUG-cc-pVDZ level of theory.

cc-pVDZ level of theory using the PCM[59,60] along with the geometries optimized at the same level of theory in gas phase. Point charges located at the atomic sites were obtained at the B3LYP/AUG-CC-pVDZ level of theory by surface molecular electrostatic potential (MEP) fitting using the CHelpG algorithm[61] and by partitioning the total electron density distribution employing the Mulliken scheme.[62]

Genuineness of the calculated transition states was confirmed by visually examining the vibrational modes related to the imaginary frequencies and applying the condition that these connected the corresponding reactant and product complexes properly. Genuineness of the optimized transition states was further ensured by intrinsic reaction coordinate (IRC) calculations.[63] For all the optimized structures, zero point energy (ZPE)-corrected total energies and the corresponding Gibbs free energies at 298.15 K were obtained at the B3LYP/AUG-cc-pVDZ and B3PW91/AUG-cc-pVDZ levels in gas phase. ZPE-corrected total energies and the corresponding Gibbs free energies at 298.15 K were also obtained at the BHandHLYP/AUG-cc-pVDZ level for all the structures of Figure 1. The gas phase ZPE corrections and thermal energy corrections giving Gibbs free energies were considered to be valid for the corresponding total energies obtained at the B3LYP/AUG-cc-pVDZ, B3PW91/AUG-cc-pVDZ, and MP2/AUG-cc-pVDZ levels of theory in aqueous media also. All the calculations were performed employing the Windows versions of Gaussian 98 (G98W)[64] and Gaussian 03 (G03W)[65] programs. For visualization of optimized structures and vibrational modes, the GaussView program[66] was employed.

3. Results and Discussion

There are five different possible mechanisms of reactions between $NO_2^{\cdot}$ with $G^{\cdot+}$ leading to the formation of 8-nitro$G^{\cdot+}$ as shown in Figures 1−3. Two different mechanisms leading to the formation of 8-nitro$G^{\cdot+}$ are shown in each of the Figures 2 and 3. One or two water molecules play catalytic roles in these reactions. Three different reactant complexes denoted by RC1, RC2, and RC3 are involved in the different reaction mechanisms, and in each case the same stable product 8-nitro$G^{\cdot+}$ complexed with one or two water molecules is formed. Gibbs free energy changes corresponding to the barrier and released energies (kcal/mol) obtained at the MP2/AUG-cc-pVDZ level of theory are presented in the different schemes. Net CHelpG and Mulliken charges associated with the different moieties and some optimized geometrical parameters of the transition states, intermediate, and product complexes obtained at B3LYP/AUG-cc-pVDZ level in gas phase are also given in the Figures 1−3. The calculated ZPE-corrected barrier energies and the corresponding Gibbs free energy changes involved in the various steps of the reactions (Figures 1−3) obtained at the different levels of theory in gas phase and aqueous media are presented in Tables 1−3.

Figure 1 involves the reactant complex RC1, intermediate complex IC1, transition states TS1, TS2 and the product complex PC1 which is a complex of 8-nitro$G^{\cdot+}$ with one water molecule (Figure 1). In RC1, the CHelpG charges associated with $G^{\cdot+}$, $NO_2^{\cdot}$, and H_2O were found to be 1.06, −0.03, −0.03, respectively while those associated with the 8-nitroguanine moiety and H_2O in PC1 were found to be 1.0 and 0.0, respectively. Thus the +1 charge of the cation is localized mostly on the 8-nitroguanine moiety in both RC1 and PC1. The positive charge of the cation is delocalized at TS1 and both the 8-nitroguanine moiety and H_2O have a CHelpG charge of 0.5 each. According to Mulliken charges, the 8-nitroguanine moiety is considerably more positively charged in both RC1 and TS1 than what is obtained by the CHelpG charges. The CHelpG charges should be considered to be more reliable than the Mulliken charges since the former are obtained by fitting to surface MEP values.

In RC1, the $NO_2^{\cdot}$ group is located near the C8 site of $G^{\cdot+}$ above the ring plane while the H_2O molecule is located near the H9 atom. At TS1, the nitro group is attached to C8 and its plane is only slightly away from the ring plane while the H8 atom is located between C8 and the O10 atom of the water molecule (Figure 1). We note that a drastic change occurs in the positions of the nitro group and the water molecule in going from RC1 to TS1 (Figure 1). A visual examination of the vibrational mode corresponding to the imaginary frequency of TS1 as well as IRC calculations revealed that in this case mainly the H8 atom moves between the C8 and O10 atoms. Thus the vibrational motion corresponding to the imaginary frequency of TS1 does not exhibit the large structural change involved in going from RC1 to TS1. This large structural change can occur in two ways: (i) There may be another transition state between RC1 and TS1, or (ii) the nitro group and the water molecule mentioned above move from their respective positions at RC1 to higher total energy positions that are connected by the above-mentioned vibrational motion at TS1, due to the energy supplied to the system. In (ii), there would be no barrier between this point lying on the potential energy surface (PES) corresponding to the higher total energy positions of the nitro group and the water molecule and the point that corresponds to RC1. Our analysis revealed that the present situation belongs to the category of (ii) as discussed below.

Geometry optimization searching for a minimum on the PES was performed starting from TS1 (Figure 1). The total SCF energies obtained at the different cycles of this geometry optimization calculation in gas phase at the B3LYP/AUG-cc-pVDZ level of theory are shown in Figure S1 (Supporting Information). This figure presents a curve on the PES along

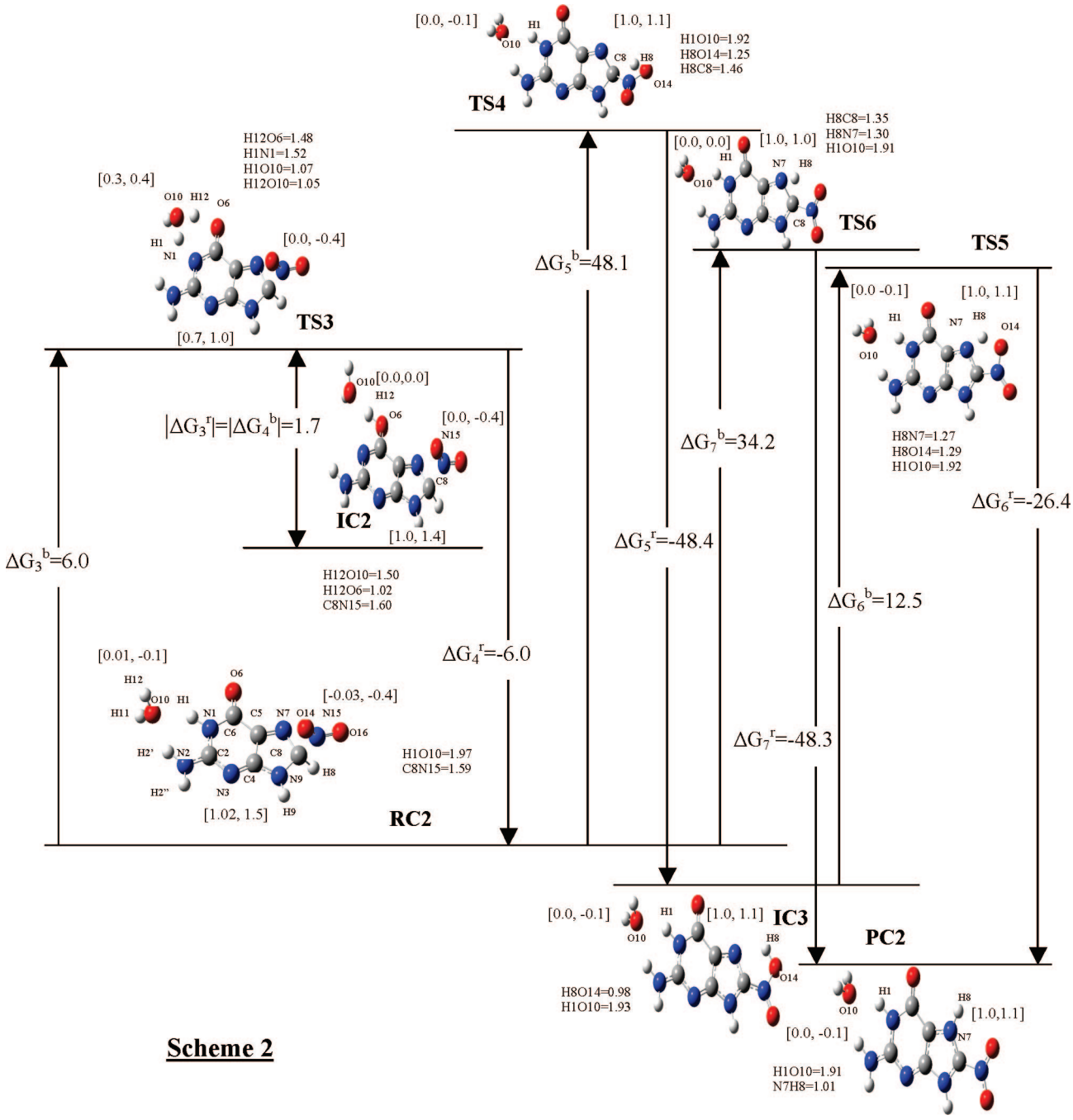

Figure 2. Reactant complex (RC2), intermediate complexes (IC2, IC3), product complex (PC2), and transition states (TS3, TS4, TS5, TS6) involved in the reaction of $NO_2^{\cdot}$ at the C8 site of $G^{\cdot+}$ in the presence of a water molecule placed near the H1 atom of $G^{\cdot+}$. Gibbs free energy changes at 298.15 K (kcal/mol), CHelpG and Mulliken charges (first and second, respectively, in the brackets) associated with different moieties obtained at the MP2/AUG-cc-pVDZ level of theory in aqueous media are given. Certain optimized interatomic distances (Å) are also given. The locations of different structures in terms of energy values are not to scale.

which the geometry optimization proceeds through the various cycles. Structures of the system and the corresponding relative total energies are given at some selected points on this curve. The point labeled A on this curve (Figure S1 in Supporting Information) is a few steps away from TS1 while the point labeled E corresponds to RC1. This curve is not expected to be unique as it may depend to some extent on the details of the optimization procedure employed. However, it seems to have certain features that are not expected to depend on the optimization procedure significantly, and are quite informative as discussed below.

The curve shown in Figure S1 (Supporting Information) has four noticeable regions, two of which are steep while the other two are nearly flat. It shows that the movement of the water molecule from near H9 to near H8 (from point E to point B in Figure S1 in Supporting Information, corresponding to breaking of the hydrogen bond involving H9 and the oxygen atom of the water molecule) is associated with a change of total energy ($\Delta E'$) of the system by ~5 kcal/mol. Further, it suggests that the system can move from the point E (RC1) to near point A along the curve shown here where it would acquire an appropriate geometry for the reaction to occur without encountering any transition state with an increase in the total energy ($\Delta E''$) by ~7 kcal/mol as obtained at the B3LYP/AUG-cc-pVDZ level of theory. The values of $\Delta E'$ and $\Delta E''$ are only approximate estimates of the corresponding energy differences.

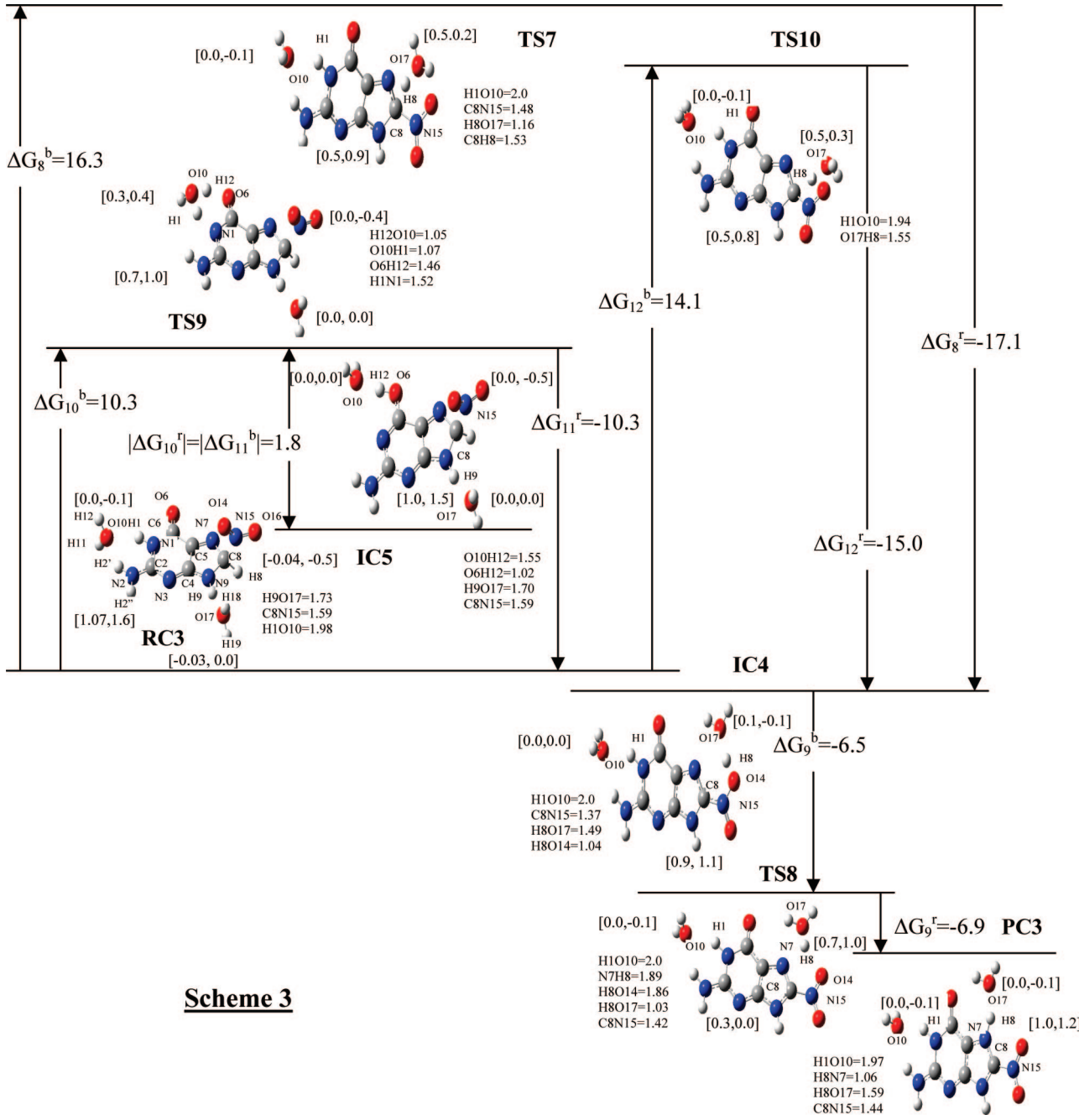

Figure 3. Reactant complex (RC3), intermediate complexes (IC4, IC5), product complex (PC3) and transition states (TS7, TS8, TS9, TS10) involved in the reaction of $NO_2^{\cdot}$ at the C8 site of $G^{\cdot+}$ in the presence of two water molecules. Gibbs free energy changes at 298.15K (kcal/mol), CHelpG and mulliken charges (first and second, respectively, in the brackets) associated with different moieties obtained at the MP2/AUG-cc-pVDZ level of theory in aqueous media are given. Certain optimized interatomic distances (Å) are also given. The locations of different structures in terms of energy values are not to scale.

The ZPE-corrected value of the barrier energy corresponding to TS1 (ΔE_1^b) in gas phase obtained at the B3LYP/AUG-cc-pVDZ level of theory was found to be 19.7 kcal/mol with the corresponding Gibbs free energy change (ΔG_1^b) being 22.1 kcal/mol. The various other methods employed here predict somewhat different values of ΔE_1^b and ΔG_1^b in gas phase (Table 1). Figure S1 in Supporting Information and the results presented in Table 1 show that ΔE_1^b or ΔG_1^b would have two parts, the first part being required to put the structure in a right geometry (near the point A) for the reaction to occur, and the second part being the energy required to cross the barrier TS1 (from near the point A).

The ZPE-corrected barrier energy corresponding to TS1 (ΔE_1^b) is 13.5 kcal/mol, the corresponding Gibbs free energy change (ΔG_1^b) being 15.8 kcal/mol at the B3LYP/AUG-cc-pVDZ level of theory in aqueous media (Figure 1). At the MP2/AUG-cc-pVDZ level of theory in aqueous media, the values of ΔE_1^b and ΔG_1^b are appreciably less than those obtained at the B3LYP/AUG-cc-pVDZ level, that is, 10.9 and 13.2 kcal/mol, respectively. The ZPE-corrected barrier energy obtained at the B3PW91/AUG-cc-pVDZ level of theory in aqueous media was found to be 12.5 kcal/mol with the corresponding Gibbs free energy change being 14.8 kcal/mol. It is noted that the bulk aqueous medium lowers down the barrier energy (ΔE_1^b) and the corresponding Gibbs free energy change (ΔG_1^b) appreciably with respect to the corresponding values in gas phase (Table 1).

TABLE 2: ZPE-Corrected Barrier Energies (ΔE_i^b) and the Corresponding Gibbs Free Energy Changes (ΔG_i^b) ($i = 3-7$) at 298.15 K (kcal/mol) Involved in the Reaction of $NO_2^{\cdot}$ with $G^{\cdot+}$ in the Presence of a Water Molecule Placed near the H1 Atom of $G^{\cdot+}$, According to Figure 2

barrier energies and corresponding Gibbs free energy changes	gas phase					aqueous media		
	B3LYP/6-31G**	B3LYP/AUG-cc-pVDZ	B3PW91/6-31G**	B3PW91/AUG-cc-pVDZ	MP2/AUG-cc-pVDZ	B3LYP/AUG-cc-pVDZ	B3PW91/AUG-cc-pVDZ	MP2/AUG-cc-pVDZ
ΔE_3^b	13.2	14.5	12.0	12.8	15.0	5.8	4.7	4.6
ΔG_3^b	14.3	15.9	13.2	14.2	16.4	7.2	6.0	6.0
ΔE_4^b	8.3	10.9	7.6	9.5	9.6	0.8	1.4	−1.1
ΔG_4^b	10.2	13.7	9.5	11.8	12.4	3.6	2.5	1.7
ΔE_5^b	42.0	41.7	40.3	39.8	44.9	45.9	43.4	47.7
ΔG_5^b	42.4	42.1	40.7	40.2	45.3	46.0	43.9	48.1
ΔE_6^b	12.5	12.6	10.8	10.7	10.0	14.5	12.6	12.3
ΔG_6^b	12.7	12.9	11.0	10.9	10.2	14.7	12.8	12.5
ΔE_7^b	39.8	38.9	37.5	36.4	36.9	37.0	34.5	33.7
ΔG_7^b	40.1	39.4	38.0	36.9	37.4	37.5	35.0	34.2

TABLE 3: ZPE-Corrected Barrier Energies (ΔE_i^b) and the Corresponding Gibbs Free Energy Changes (ΔG_i^b) ($i = 8-12$) at 298.15 K (kcal/mol) Involved in the Reaction of $NO_2^{\cdot}$ with $G^{\cdot+}$ in the Presence of Two Water Molecules Placed near the C8 and H1 Atoms of $G^{\cdot+}$, According to Figure 3

barrier energies and corresponding Gibbs free energy changes	gas phase					aqueous media		
	B3LYP/6-31G**	B3LYP/AUG-cc-pVDZ	B3PW91/6-31G**	B3PW91/AUG-cc-pVDZ	MP2/AUG-cc-pVDZ	B3LYP/AUG-cc-pVDZ	B3PW91/AUG-cc-pVDZ	MP2/AUG-cc-pVDZ
ΔE_8^b	18.8	21.4	16.9	18.9	21.4	16.5	14.7	13.9
ΔG_8^b	21.4	23.8	19.3	21.4	23.8	18.6	17.1	16.3
ΔE_9^b	9.3	10.1	9.1	9.3	5.2	−1.6	2.3	−6.7
ΔG_9^b	9.9	10.4	9.5	9.6	5.4	−1.4	2.6	−6.5
ΔE_{10}^b	18.5	14.8	12.2	13.0	15.5	10.5	9.0	8.9
ΔG_{10}^b	20.5	16.2	13.3	14.4	16.9	11.8	10.4	10.3
ΔE_{11}^b	13.1	10.7	7.3	9.2	9.6	1.8	0.9	−0.3
ΔG_{11}^b	15.8	12.7	9.2	11.2	11.7	3.8	2.8	1.8
ΔE_{12}^b	19.8	22.2	17.9	19.8	22.2	14.8	12.7	11.7
ΔG_{12}^b	22.4	24.6	20.3	22.1	24.6	17.2	15.1	14.1

The intermediate complex IC1 is formed following TS1, where the H8 atom gets attached to the O14 atom of the $NO_2^{\cdot}$ group. The product complex PC1 is formed from IC1 through the transition state TS2 where the H8 atom moves from O14 to the N7 site of guanine. The barrier energy (ΔE_2^b) and the Gibbs free energy change (ΔG_2^b) at the second step of Figure 1 were found to be 1.3 and 1.7 kcal/mol at the B3LYP/AUG-cc-pVDZ level of theory in aqueous media the corresponding gas phase values being appreciably larger. The values of ΔE_2^b and ΔG_2^b were found at the MP2/AUG-cc-pVDZ level of theory in aqueous media to be −3.8 and −3.4 kcal/mol, respectively (Table 1). Thus the bulk solvent effect of water reduces the second barrier energy (ΔE_2^b) as well as the corresponding Gibbs free energy change (ΔG_2^b) at the B3LYP/AUG-cc-pVDZ level of theory appreciably (Table 1). We also note that the improved treatment of electron correlation at the MP2/AUG-cc-pVDZ level than that achieved at the B3LYP/AUG-cc-pVDZ level lowers down the barrier energy (ΔE_2^b) and the Gibbs free energy change (ΔG_2^b) appreciably. Since both the barrier energies (ΔE_1^b, ΔE_2^b) as well as the corresponding Gibbs free energy changes (ΔG_1^b, ΔG_2^b) are small positive or negative, formation of 8-nitro$G^{\cdot+}$ due to the reaction of $G^{\cdot+}$ with $NO_2^{\cdot}$ in aqueous media owing to the involvement of a specific water molecule located near the N7 and C8 sites (Figure 1) would occur efficiently.

Though the transition states TS1 and TS2 of scheme 1 were located at both the B3PW91/6-31G** and B3PW91/AUG-cc-pVDZ levels of theory in gas phase, the intermediate complex IC1 could not be located at these levels. Therefore, to obtain further support for validity of scheme 1 including the existence of IC1, this scheme was fully investigated at the BHandHLYP/AUG-cc-pVDZ level of theory also in gas phase. The BHandHLYP functional was used here since it has recently been shown to be one of the reliable functionals.[67] The BHandHLYP/AUG-cc-pVDZ calculations confirmed the prediction of B3LYP/6-31G** and B3LYP/AUG-cc-pVDZ calculations regarding the existence of IC1 and validity of Figure 1 discussed above (Table 1).

The possibility of direct transfer of the H8 atom from C8 to N7 involving a water molecule located in the vicinity leading to the formation of PC1, as a possible alternative to the mechanism shown in Figure 1, was examined. This type of transfer of H8 occurs in one of the mechanisms included in Figure 2, but in that case, there is no water molecule located nearby. We found that in the presence of a water molecule located in the vicinity of N7 and C8 (Figure 1), the direct transfer of H8 from C8 to N7 would not occur. It was found that when the H8 atom moves from C8 to the oxygen atom of the water molecule, the water molecule always, in turn, loses one of its hydrogen atoms to the O14 atom of the $NO_2^{\cdot}$ group forming IC1 (Figure 1). Thus the only mechanism for transfer of H8 from C8 to N7 in the presence of a water molecule located near these atoms appears to be the one shown in Figure 1. At TS2, the distances of H8 from O10, N7, and O14 are 1.02, 1.97, and 1.89 Å, respectively. Thus at TS2, an H_3O^+ is formed. The net CHelpG charge including the charge components located on the atoms of H_2O and H8 is 0.7 while the corresponding Mulliken charge is 1.0 which confirm the formation of H_3O^+ (Figure 1).

The vibrational mode of TS2 (Figure 1) corresponding to the imaginary frequency involves motion of the H_3O^+ part only. In this mode, the H_3O^+ part, remaining structurally intact, rotates

back and forth such that the H8 atom gets hydrogen bonded with the N7 and O14 atoms alternately. Thus, in Figure 1 H_3O^+ is formed transiently at the transition state TS2. IRC calculations confirmed that PC1 would not contain H_3O^+ as its component. Thus the reaction between $G^{\cdot+}$ and $NO_2^{\cdot}$ in the presence of a water molecule produces 8-nitro$G^{\cdot+}$ complexed with a water molecule (Figure 1). Here the water molecule acts as a catalyst through a transient formation of H_3O^+. This finding of the present study differs from that of Liu et al.[46] according to whom H_3O^+ is a component of the product.

Figure 2 involves the reactant complex RC2, intermediate complexes IC2, IC3, IC4, transition states TS3, TS4, TS5 and the product complex PC2 that is a complex of 8-nitro$G^{\cdot+}$ with one water molecule located near the H1 and O6 sites of guanine. The water molecule was placed in this scheme near the H1 and O6 sites as it may catalyze keto−enol tautomerism of guanine. It appeared to be desirable to examine how the barrier energy to binding of the $NO_2^{\cdot}$ group at the C8 site of guanine is affected in this mode of interaction of the water molecule with the $G^{\cdot+}$−$NO_2^{\cdot}$ complex. In RC2, the CHelpG charges associated with $G^{\cdot+}$, H_2O, and $NO_2^{\cdot}$ are 1.02, 0.01, −0.03 while the corresponding Mulliken charges are 1.5, −0.1, and −0.4, respectively. Thus the $G^{\cdot+}$ moiety does not lose its positive charge on formation of the complex RC2. The intermediate complex IC2 of the enol form of $G^{\cdot+}$, H_2O, and $NO_2^{\cdot}$ formed through TS3 is less stable than the corresponding complex (RC2) involving the keto form of $G^{\cdot+}$ by 4.3 kcal/mol (Figure 2). Further, formation of IC2 from RC2 would involve a barrier of 6 kcal/mol as obtained at the MP2/AUG-cc-pVDZ level of theory in aqueous media. As IC2 is appreciably less stable than RC2, the reaction would proceed mainly from RC2, and the role of IC2 would be important in this regard. If IC2 is formed from RC2, it can convert back to RC2 overcoming a barrier (ΔG_4^{b}) of 1.7 kcal/mol (Figure 2).

From RC2, going through the transition state TS4, the intermediate complex IC3 is formed, and from IC3, going through the transition state TS5, the final product PC2 is formed. At TS4, the H8 atom gets detached from C8 and moves toward the O14 atom of the $NO_2^{\cdot}$ group, the nitrogen atom of which is ready to get attached to C8. Bonding of H8 to O14 and that of the $NO_2^{\cdot}$ group to C8 are accomplished at IC3. The ZPE-corrected barrier energy (ΔE_5^{b}) involved at this reaction step is quite high, that is, 45.9 kcal/mol, the corresponding Gibbs free energy change (ΔG_5^{b}) being 46.0 kcal/mol at the B3LYP/AUG-cc-pVDZ level of theory in aqueous media. At the MP2/AUG-cc-pVDZ level of theory, the values of ΔE_5^{b} and ΔG_5^{b} are found to be 47.7 and 48.1 kcal/mol, respectively. At the B3PW91/AUG-cc-pVDZ level of theory, the ZPE-corrected barrier energy is found to be 43.4 kcal/mol with the corresponding Gibbs free energy change being 43.9 kcal/mol. At TS5, the H8 atom bonded to O14 moves toward N7. The ZPE-corrected barrier energy (ΔE_6^{b}) involved at this step is 14.5 kcal/mol while the corresponding Gibbs free energy change (ΔG_6^{b}) is 14.7 kcal/mol at the B3LYP/AUG-cc-pVDZ level of theory in aqueous media. At the MP2/AUG-cc-pVDZ level, ΔE_6^{b} and ΔG_6^{b} are reduced to 12.3 and 12.5 kcal/mol, respectively, in aqueous media.

There is another possible mechanism for the formation of PC2 from RC2 as shown in Figure 2. In this alternative mechanism, PC2 is formed from RC2 through the transition state TS6. In this case, the H8 atom moves directly from C8 to N7 without getting bonded to O14. The ZPE-corrected barrier energy (ΔE_7^{b}) corresponding to the transition state TS6 is 37.0 kcal/mol while the corresponding Gibbs free energy change (ΔG_7^{b}) is 37.5 kcal/mol at the B3LYP/AUG-cc-pVDZ level of theory in aqueous media. The values of ΔE_7^{b} and ΔG_7^{b} in aqueous media were found at the MP2/AUG-cc-pVDZ level of theory to be 33.7 and 34.2 kcal/mol, respectively. At the B3PW91/AUG-cc-pVDZ level of theory, the values of ΔE_7^{b} and ΔG_7^{b} were found to be 34.5 and 35.0 kcal/mol, respectively. Since ΔG_7^{b} is less than ΔG_5^{b} by approximately 13.9 kcal/mol in aqueous media as obtained at the MP2/AUG-cc-pVDZ level of theory, the reaction through TS6 would be preferred over that through TS4 and TS5.

Figure 3 involves the reactant complex RC3, intermediate complex IC4, transition states TS7 and TS8, and the product complex PC3. PC3 is a complex of 8-nitro$G^{\cdot+}$ with two water molecules, one of them being located near the H8 (bonded to N7) and O6 sites while the other is located near the H1 site of guanine. At RC3, the $NO_2^{\cdot}$ group, is located near C8 above the ring plane. The CHelpG and Mulliken charges show that the positive charge of the cation continues to be located on the guanine moiety. In going from RC3 to TS7, the water molecule moves from near H9 to near H8 while the $NO_2^{\cdot}$ group gets bonded to C8 lying nearly in the ring plane. At TS7, the positive CHelpG charge is equally distributed on the water molecule that is hydrogen-bonded to H8 and the 8-nitroguanine-like moiety. The large change that occurs in the positions of the H_2O molecule and the $NO_2^{\cdot}$ group in going from RC3 to TS7 is similar to what has been discussed earlier with regard to RC1 and TS1 of Figure 1. We studied the change of total energy that occurred during the process of optimization in this case also, and it was found to be similar to what has been discussed earlier with regard to Figure 1. The barrier energy involved in going from RC3 to TS7 (ΔE_8^{b}) is found to be 21.4 kcal/mol in gas phase and 16.5 kcal/mol in aqueous media as obtained at the B3LYP/AUG-cc-pVDZ level of theory, the corresponding Gibbs free energy changes being 23.8 and 18.6 kcal/mol, respectively (Table 3). Thus we find that in going from gas phase to aqueous media, the values of ΔE_8^{b} and ΔG_8^{b} are reduced by ∼5 kcal/mol. At the MP2/AUG-cc-pVDZ level of theory, the reductions in the values of ΔE_8^{b} and ΔG_8^{b} in going from gas phase to aqueous media is even more pronounced (∼7.5 kcal/mol) (Table 3).

The intermediate complex IC4 is formed from TS7 and the product complex PC3 is formed from IC4 through the transition state TS8 (Figure 3). The structures of IC1 and IC4, those of the transition states TS2 and TS8, and those of the product complexes PC1 and PC3 of the Figures 1 and 3 are similar except that in each of IC4, TS8, and PC3 (Figure 3), there is an additional hydrogen bonded water molecule located near the H1 site (Figures 1 and 3). The barrier energy (ΔE_9^{b}) and the corresponding Gibbs free energy change (ΔG_9^{b}) corresponding to TS8 were found at the B3LYP/AUG-cc-pVDZ level of theory in aqueous media to be −1.6 and −1.4 kcal/mol, respectively. At the MP2/AUG-cc-pVDZ level of theory, these energies are further lowered down to −6.7 and −6.5 kcal/mol, respectively (Table 3). Negative barrier energy and Gibbs free energy change imply that the corresponding reaction step would be barrierless. We can evaluate the role of the water molecule located near the H1 site by a comparison of the corresponding barrier energies of Figures 1 and 3. The barrier energy ΔE_2^{b} and the Gibbs free energy change (ΔG_2^{b}) of Figure 1 correspond to the barrier energy ΔE_9^{b} and the Gibbs free energy change (ΔG_9^{b}) of Figure 3, respectively. Although the water molecule located near H1 is not directly involved in the reaction, its hydrogen bonding with the H1 atom lowers down the second barrier energy (ΔE_9^{b}) such that the corresponding step of the reaction in Figure 3 becomes barrierless. However, the presence of the same water molecule increases the first barrier energy from 10.9

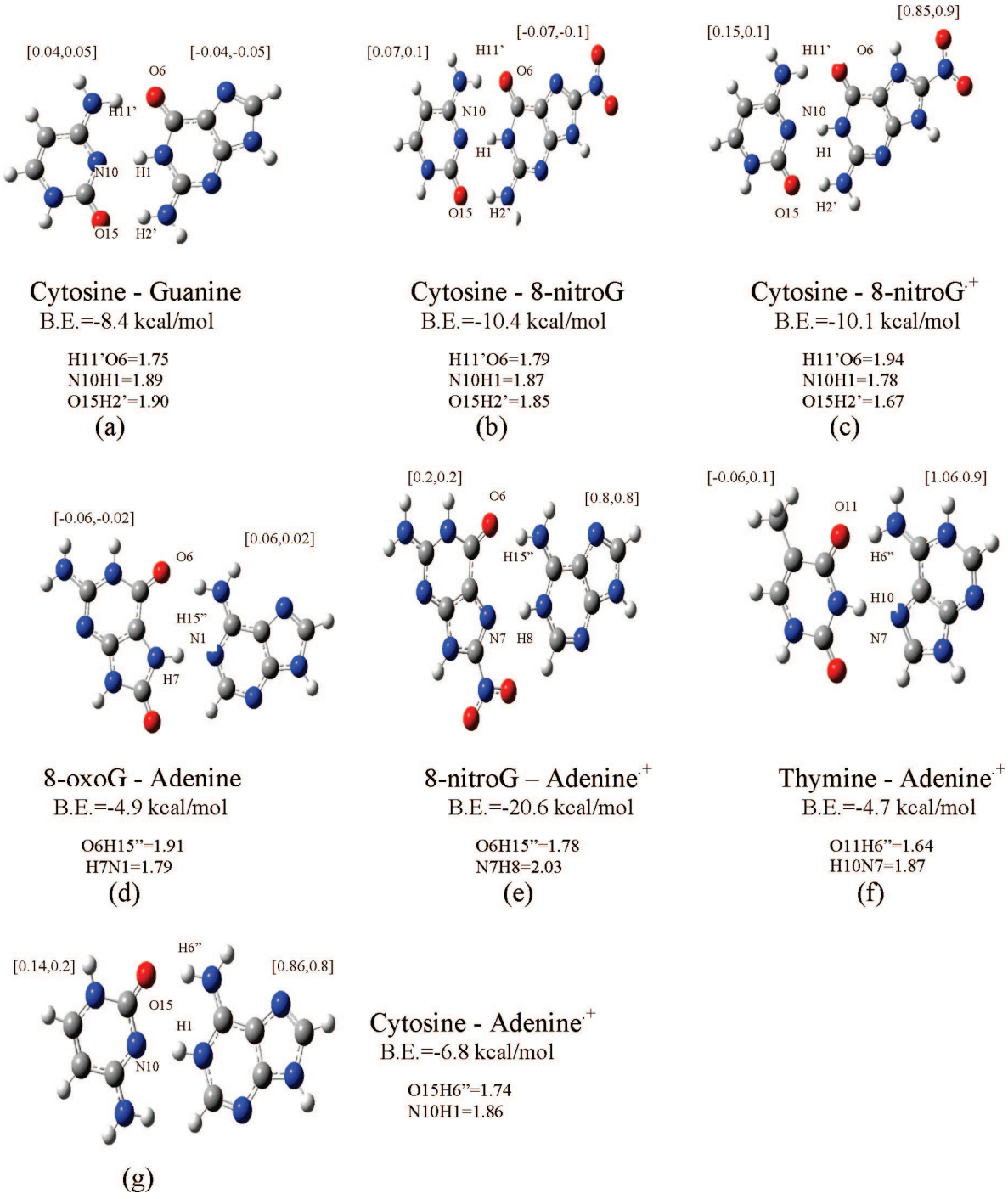

Figure 4. ZPE-corrected binding energies of different hydrogen bonded pairs obtained at the B3LYP/AUG-cc-pVDZ level of theory in aqueous media. CHelpG and Mulliken charges (first and second respectively in the brackets) associated with different moieties obtained at the B3LYP/6-31G** of theory in gas phase are also given.

kcal/mol (ΔE_1^b in Figure 1) to 13.9 kcal/mol (ΔE_8^b in Figure 3) with the corresponding Gibbs free energy changes being 13.2 and 16.3 kcal/mol, respectively, as obtained at the MP2/AUG-cc-pVDZ level of theory in aqueous media.

Figure 3 includes another possible mechanism for the formation of PC3 from RC3 via the transition states TS9, TS10, and TS8 and the intermediate IC4 (Figure 3). Because of geometrical rearrangements, RC3 (keto form of guanine) is converted to the enolic form (IC5) via the transition state TS9 with barrier energy (ΔE_{10}^b) 8.9 kcal/mol, the corresponding Gibbs free energy change (ΔG_{10}^b) being 10.3 kcal/mol at the MP2/AUG-cc-pVDZ level of theory in aqueous media. At the B3PW91/AUG-cc-pVDZ level of theory, the values of ΔE_{10}^b and ΔG_{10}^b in aqueous media were found to be 9.0 and 10.4, kcal/mol respectively (Table 3). IC5 can convert to RC3 overcoming a barrier of 1.8 kcal/mol. As RC3 is much more stable than IC5, the reaction would mainly proceed from it (Figure 4). The ZPE-corrected barrier energy (ΔE_{12}^b) corresponding to the transition state TS10 was found to be 14.8 kcal/mol with the corresponding Gibbs free energy change (ΔG_{12}^b) being 17.2 kcal/mol at the B3LYP/AUG-cc-pVDZ level of theory in aqueous media (Table 3). At the MP2/AUG-cc-pVDZ level of theory in aqueous media, the values of ΔE_{12}^b and ΔG_{12}^b were found to be 11.7 and 14.1 kcal/mol, respectively. At the B3PW91/AUG-cc-pVDZ level of theory, the values of ΔE_{12}^b and ΔG_{12}^b in aqueous media were found to be 12.7 and 15.1 kcal/mol, respectively.

From the point of view of structural changes, there is a good deal of similarity between the steps that follow RC2 through the transition states TS4 and TS5 up to the formation of PC2 in Figure 2 and those that follow RC3 through the transition states TS8 and TS10 up to the formation of PC3 in Figure 3. Through these steps of the two Figures, the H8 atom moves from the C8 site of guanine to the N7 site. The main difference between Figures 2 and 3 is that while there is only one water molecule (located near the H1 site) in Figure 2, there are two water molecules (located near the H1 and N7 sites) in Figure 3, due to which the corresponding barrier energies are different. Thus while the barrier energy ΔE_6^b in aqueous media obtained at the MP2/AUG-cc-pVDZ level of theory is 12.3 kcal/mol in Figure 2, the corresponding barrier energy (ΔE_9^b) is negative (−6.7 kcal/mol) in Figures 3. The Gibbs free energy changes corresponding to these barrier energies in aqueous media are 12.5 and −6.5 kcal/mol, respectively. A drastic change in the barrier energy or the Gibbs free energy change occurs in going from Figure 2 to Figure 3 due to the catalytic involvement of the water molecule located near the C8 site of guanine.

In an experimental situtation, there would be several water molecules hydrogen bonded with the $G^{\cdot+}$-$NO_2^{\cdot}$ complex. Therefore, from the point of view of modeling the experimental situation, Figure 3 would be more realistic than Figures 1 and 2, since two water molecules are considered in the former Figure while only one water molecule is considered in each of the latter two Figures. The various water molecules hydrogen bonded with the $G^{\cdot+}$-$NO_2^{\cdot}$ complex would affect the barrier energies to different extents but the main effect in this context would be caused by the water molecule present near the C8 site. The solvent effect of bulk water also plays an important role in this context. On the whole, the present study shows that 8-nitro$G^{\cdot+}$ would be formed with low barrier energies due to the reaction of $G^{\cdot+}$ and $NO_2^{\cdot}$ in aqueous media.

4. Biological Significance

In order to be able to understand the possible biological consequences of formation of 8-nitro$G^{\cdot+}$ due to reaction between $G^{\cdot+}$ and $NO_2^{\cdot}$ in biological media, we carried out calculations on several hydrogen bonded pairs involving 8-nitro$G^{\cdot+}$ and the normal DNA bases adenine (A), thymine (T), guanine (G), and cytosine (C). Certain other base pairs were also studied for comparison. In these calculations, geometries of hydrogen bonded pairs were optimized at the B3LYP/6-31G** level of theory in gas phase. Solvation of the pairs in aqueous media was treated by single point energy calculations at the B3LYP/6-31G** and B3LYP/AUG-cc-pVDZ levels using the PCM.[59,60] The calculated ZPE-corrected binding energies (defined as ZPE-corrected total energies of hydrogen bonded pairs, sums of ZPE-corrected total energies of the corresponding individual constituents) of the different hydrogen-bonded pairs obtained at the different levels of theory in gas phase and aqueous media are presented in Table 4. A negative binding energy implies that the pair under consideration is stable. Optimized structures of the pairs along with certain important interatomic distances and calculated binding energies in aqueous media at the B3LYP/AUG-cc-pVDZ level of theory are presented in Figure 4. The different normal and abnormal base pairs shown in this figure are as follows: (a) Normal Watson−Crick C-G base pair, (b) Watson−Crick type pair that would be formed when guanine in the C-G base pair is replaced by neutral 8-nitroguanine, (c) Watson−Crick type C-8-nitro$G^{\cdot+}$ pair, (d) 8-oxoG-A pair that is known to cause lethal mutations,[13] (e) 8-nitro$G^{\cdot+}$-A pair that has been converted to 8-nitroG-$A^{\cdot+}$ pair, (f) T-$A^{\cdot+}$ pair (the normal Watson−Crick type pairing between $A^{\cdot+}$ and T cannot take place), and (g) C-$A^{\cdot+}$ pair that can be obtained by replacing G in the C-G base pair by $A^{\cdot+}$.

TABLE 4: ZPE-Corrected Binding Energies of Different Hydrogen-Bonded Pairs Obtained at Different Levels of Theory in Gas Phase and Aqueous Media

	binding Energies		
	gas phase	aqueous media	
hydrogen-bonded pairs[a]	B3LYP/6-31G**	B3LYP/6-31G**	B3LYP/AUG-cc-pVDZ
Cytosine−Guanine	−28.9	−13.4	−8.4
Cytosine−8-nitroG	−30.4	−13.3	−10.4
Cytosine−8-nitro$G^{\cdot+}$	−74.2	−14.5	−10.1
8-oxoG−Adenine	−15.9	−8.0	−4.9
8-nitroG−$Adenine^{\cdot+}$	−83.8	−24.7	−20.6
Thymine−$Adenine^{\cdot+}$	−23.5	−7.9	−4.7
Cytosine−$Adenine^{\cdot+}$	−37.6	−11.5	−6.8

[a] Structures of the different hydrogen bonded pairs are shown in Figure 4.

In the 8-nitro$G^{\cdot+}$-A pair (e), the proton that was initially attached to the N7 site of guanine has moved to the N1 site of adenine. Net CHelpG and Mulliken charges located on the two hydrogen bonded molecules in each case were found to be similar. The CHelpG charges located on adenine and 8-nitro$G^{\cdot+}$ in (e) were found to be 0.8 and 0.2, respectively. Thus the 8-nitro$G^{\cdot+}$-A pair has been converted to 8-nitroG-$A^{\cdot+}$ pair. In the C-8-nitro$G^{\cdot+}$ base pair (c), the CHelpG charges located on cytosine and 8-nitro$G^{\cdot+}$ were found to be 0.15 and 0.85, respectively. Thus in this case, there is a small positive charge transfer from 8-nitro$G^{\cdot+}$ to C. In (f), the CHelpG charges on T and $A^{\cdot+}$ were found to be −0.06 and 1.06, respectively, while in (g) the charges on C and $A^{\cdot+}$ were found to be 0.14 and 0.86, respectively. Thus in (f) and (g), adenine is in the cationic radical form.

We find that the magnitudes of binding energies of the different pairs are strongly reduced in going from gas phase to aqueous media (Table 4). The magnitudes of binding energies are further reduced in going from B3LYP/6-31G** level to B3LYP/AUG-cc-pVDZ level of theory in aqueous media for all the pairs (Table 4). The 8-oxoG-A base pair (d) is observed experimentally.[68] The negative calculated binding energy of this pair conforms to the experimental observation. The binding energy of the 8-nitroG-$A^{\cdot+}$ pair (e) in aqueous media is much larger than those of the other pairs (Table 4). In fact, the binding energy of the 8-nitroG-$A^{\cdot+}$ pair (e) is more than double of that of the normal C-G base pair (a). The binding energies of the C-8-nitroG, C-8-nitro$G^{\cdot+}$ and normal C-G base pairs are comparable. As the 8-nitroG-$A^{\cdot+}$ pair (e) is much more stable than the C-8-nitro$G^{\cdot+}$ pair, the former would be formed preferentially to the latter during DNA replication consequent upon formation of 8-nitro$G^{\cdot+}$ following production of $G^{\cdot+}$ and its reaction with $NO_2^{\cdot}$. Further, if the adenine radical cation ($A^{\cdot+}$) formed in (e) is separated from 8-nitroG due to interaction of the two partners with other neutral molecules or ions, it can make two abnormal pairs during DNA replication as shown in (f) and (g) (Figure 4). In (f), the pairing of $A^{\cdot+}$ with thymine involves the N7 site of the five-membered ring of the former which does not occur in the normal A-T base pair. Similarly, occurrence of the C-$A^{\cdot+}$ pair (g) in DNA is abnormal. The above discussion shows that occurrence of 8-nitro$G^{\cdot+}$ in place of guanine in DNA would be very likely to cause mutation.

5. Conclusions

We arrive at the following conclusions from the present study:

1. The reaction between $G^{\cdot+}$ and $NO_2^{\cdot}$ in the presence of water molecules placed at appropriate positions leads to the formation of 8-nitro$G^{\cdot+}$ complexed with the water molecules. The water molecules serve as catalysts and are not essential constituents of the reaction. 8-NitroG complexed with H_3O^+ would be formed transiently at a transition state in the presence of a water molecule placed near the C8 site of $G^{\cdot+}$, but H_3O^+ would not be produced as a component of the stable product.

2. The solvent effect of bulk water and that of the specific water molecules play important roles in lowering down several barrier energies. As a result, several steps of the reaction between $G^{\cdot+}$ and $NO_2^{\cdot}$ become barrierless.

3. Formation and incorporation of 8-nitro$G^{\cdot+}$ in place of guanine in DNA can cause mutation.

Acknowledgment. The authors are thankful to the University Grants Commission (New Delhi) and the Council of Scientific and Industrial Research (New Delhi) for financial support. Authors are also thankful to Mr. P. K. Shukla for discussion.

Supporting Information Available: This material is available free of charge via the Internet at http://pubs.acs.org.

References and Notes

(1) Wiseman, H.; Halliwell, B. *Biochem. J.* **1996**, *313*, 17.
(2) Squadrito, G. L.; Pryor, W. A. *Free Radical Biol. Med.* **1998**, *25*, 392.
(3) Halliwell, B.; Guteridge, J. M. C. Free Radicals In Biology and Medicine; Oxford Science Publications: Oxford, U.K., 1999.
(4) Pryor, W. A.; Squadrito, G. L. *Am. Physiol. J.* **1995**, *268*, L699.
(5) Dedon, P. C.; Tannenbaum, S. R. *Arch. Biochem. Biophys.* **2004**, *423*, 12.
(6) Ischiropoulos, H. *Arch. Biochem. Biophys.* **1998**, *356*, 1.
(7) Radi, R.; Beckman, J. S.; Bush, K. M.; Freeman, B. A. *Arch. Biochem. Biophys.* **1991**, *288*, 481.
(8) Beckman, J. S.; Beckman, T. W.; Chen, J.; Marshal, P. M.; Freeman, B. A. *Proc. Natl. Acad. Sci. U.S.A.* **1990**, *87*, 1620.
(9) Tretyakova, N. Y.; Burney, S.; Pamir, B.; Wishnok, J. S.; Dedon, P. C.; Wogan, G. N.; Tannenbaum, S. R. *Mutat. Res.* **2000**, *447*, 287.
(10) King, P. A.; Anderson, V. E.; Edwards, J. O.; Gustafson, G.; Plumb, R. C.; Suggs, J. W. *J. Am. Chem. Soc.* **1992**, *114*, 5430.
(11) Munk, B. H.; Burrows, C. J.; Schlegel, H. B. *J. Am. Chem. Soc.* **2008**, *130*, 5245.
(12) Jena, N. R.; Mishra, P. C. *J. Comput. Chem.* **2007**, *28*, 1321.
(13) Reynisson, J.; Steenken, S. J. *Mol. Struct.* **2005**, *723*, 29.
(14) Milligan, J. R.; Aguilera, J. A.; Ly, A.; Tran, N. Q.; Hoang, O.; Ward, J. F. *Nucl. Acid Res.* **2003**, *31*, 6258.
(15) Radom, C. T.; Banerjee, A.; Verdine, G. L. *J. Biol. Chem.* **2007**, *282*, 9182.
(16) David, S. S.; O'Shea, V. L.; Kundu, S. *Nature* **2007**, *447*, 941.
(17) Bruner, S. D.; Norman, D. P. G.; Verdine, G. C. *Nature* **2000**, *403*, 859.
(18) Neely, W. L.; Essigmann, J. M. *Chem. Res. Toxicol.* **2006**, *19*, 491.
(19) Suzuki, N.; Yasui, M.; Geacintov, N. E.; Shafirvoich, V.; Shibutani, S. *Biochemistry* **2005**, *44*, 9238.
(20) Bera, P. P.; Schaefer, H. F., III. *Proc. Natl. Acad. Sci. U.S.A.* **2005**, *102*, 6698.
(21) Cai, Z.; Sevilla, M. D. *Radiat. Res.* **2003**, *159*, 411.
(22) Venkateswarlu, D.; Leszczynski, J. J. *Comput.-Aided Mol. Des.* **1998**, *12*, 373.
(23) Mantz, Y. A.; Gerard, H.; Iftimie, R.; Martyna, G. J. *J. Phys. Chem. B* **2006**, *110*, 13523.
(24) Jalkanen, K. J.; Degtyarenko, I. M.; Nieminen, R. M.; Cao, X.; Nafie, L. A.; Zhu, F.; Barron, L. D. *Theor. Chem. Acc.* **2008**, *119*, 191.
(25) Han, W. G.; Jalkanen, K. J.; Elstner, M.; Suhai, S. *J. Phys. Chem. B* **1998**, *102*, 2587.
(26) Deng, Z.; Polavarapu, P. L.; Ford, S. J.; Hecht, L.; Barron, L. D.; Ewig, C. S.; Jalkanen, K. J. *J. Phys. Chem.* **1996**, *100*, 2025.
(27) Tajkhorshid, E.; Jalkanen, K. J.; Suhai, S. *J. Phys. Chem. B* **1998**, *102*, 5899.
(28) Degtyarenko, I. M.; Jalkanen, K. J.; Gurtovenko, A. A.; Nieminen, R. M. *J. Phys. Chem. B* **2007**, *111*, 4227.
(29) Jalkanen, K. J.; Suhai, S. *Chem. Phys.* **1996**, *208*, 81.
(30) Lymar, S. V.; Hurst, J. K. *Inorg. Chem.* **1998**, *37*, 294.
(31) Van der Vliet, A.; O'Neill, C. A.; Halliwell, B.; Cross, C. E.; Kaur, H. *FEBS Lett.* **1999**, *339*, 89.
(32) Radi, R.; Cosgrove, T. P.; Beckman, J. S.; Freeman, B. A. *Biochem. J.* **1993**, *290*, 51.
(33) Gow, A.; Duran, D.; Thom, S. R.; Ischiropoulos, H. *Arch. Biochem. Biophys.* **1996**, *333*, 42.
(34) Uppu, R. M.; Cueto, R.; Squadrito, G. L.; Salgo, M. G.; Pryor, W. A. *Free Radical Biol. Med.* **1996**, *21*, 407.
(35) Denicola, A.; Freeman, B. A.; Trujillo, M.; Radi, R. *Arch. Biochem. Biophys.* **1996**, *333*, 49.
(36) Lymar, S. V.; Jiang, Q.; Hurst, J. K. *Biochemistry* **1996**, *35*, 7855.
(37) Lymar, S. V.; Hurst, J. K. *J. Am. Chem. Soc.* **1995**, *117*, 8867.
(38) Lymar, S. V.; Hurst, J. K. *Chem. Res. Toxicol.* **1996**, *9*, 845.
(39) Goldstein, S.; Czapski, G. *J. Am. Chem. Soc.* **1998**, *120*, 3458.
(40) Squadrito, G. L.; Pryor, W. A. *Chem. Res. Toxicol.* **2002**, *15*, 885.
(41) Lee, Y. A.; Yun, B. H.; Kim, S. K.; Margolin, Y.; Dedon, P. C.; Geacintov, N. E.; Shafirovich, V. *Chem.—Eur. J.* **2007**, *13*, 4571.
(42) Shukla, P. K.; Mishra, P. C. *J. Phys. Chem. B* **2008**, *112*, 4779.
(43) Augusto, A.; Bonini, M. G.; Amanso, A. M.; Linares, E.; Santos, C. C. X.; Menezes, L. D. *Free Radical Biol. Med.* **2002**, *32*, 841.
(44) Misiaszek, R.; Crean, C.; Geacintov, N. E.; Shafirovich, V. *J. Am. Chem. Soc.* **2005**, *127*, 2191.
(45) Niles, J. C.; Wishnok, J. S.; Tannenbaum, S. R. *Nitric Oxide* **2006**, *14*, 109.
(46) Liu, N.; Ban, F.; Boyd, R. J. *J. Phys. Chem. A* **2006**, *110*, 9908.
(47) Mishra, S. K.; Mishra, P. C. *J. Comput. Chem.* **2002**, *23*, 530.
(48) Shukla, M. K.; Mishra, S. K.; Kumar, A.; Mishra, P. C. *J. Comput. Chem.* **2000**, *21*, 826.
(49) Kobayashi, K.; Tagwa, S. *J. Am. Chem. Soc.* **2003**, *125*, 10213.
(50) Candeiss, L.; Steenken, S. *J. Am. Chem. Soc.* **1993**, *115*, 2437.
(51) Schuster, G. B.; Landman, U. *Top. Curr. Chem.* **2004**, *236*, 139.
(52) Gasper, S. M.; Schuster, G. B. *J. Am. Chem. Soc.* **1997**, *119*, 12762.
(53) Nunez, M.; Hall, D. B.; Barton, J. K. *Chem. Biol.* **1999**, *6*, 85.
(54) Steenken, S.; Jovanovic, S. V. *J. Am. Chem. Soc.* **1997**, *119*, 617.
(55) Das, P.; Schuster, G. B. *Proc. Natl. Acad. Sci. U.S.A.* **2005**, *102*, 14227.
(56) Becke, A. D. *J. Chem. Phys.* **1993**, *98*, 5648.
(57) Lee, C.; Yang, W.; Parr, R. G. *Phys. Rev. B* **1988**, *37*, 785.
(58) Schlegel, H. B. *J. Comput. Chem.* **1982**, *3*, 214.
(59) Miertus, S.; Tomasi, *J. Chem. Phys.* **1982**, *65*, 239.
(60) Miertus, S.; Scrocco, E.; Tomasi, *J. Chem. Phys.* **1981**, *55*, 117.
(61) Breneman, C. M.; Wiberg, K. B. *J. Comput. Chem.* **1990**, *11*, 361.
(62) Mulliken, R. S. *J. Chem. Phys.* **1955**, *23*, 1833, 1841, 2338, 2343.
(63) Gonzalez, C.; Schlegel, H. B. *J. Chem. Phys.* **1989**, *90*, 2154.
(64) Frisch, M. J.; Trucks, G. W.; Schlegel, H. B.; Scuseria, G. E.; Robb, M. A.; Cheeseman, J. R.; Zakrzewski, V. G.; Montgomery, J. A., Jr.; Stratmann, R. E.; Burant, J. C.; Dapprich, S.; Millam, J. M.; Daniels, A. D.; Kudin, K. N.; Strain, M. C.; Farkas, O.; Tomasi, J.; Barone, V.; Cossi, M.; Cammy, R.; Mennucci, B.; Pomelli, C. Adamo, C.; Clifford, S.; Ochterski, J.; Petersson, G. A.; Ayala, P. Y.; Cui, Q.; Morokuma, K.; Rega, N.; Salvodar, P.; Dannenberg, J. J.; Malick, D. K.; Rabuck, A. D.; Raghavachari, K.; Foresman, J. B.; Cioslowski, J.; Ortiz, J. V.; Baboul, A. G.; Stefanov, B. B.; Liu, G.; Liashenko, A.; Piskorz, P.; Komaromi, I.; Gomperts, R.; Martin, R. L.; Fox, D. J.; Keith, T.; Al-Laham, M. A.; Peng, C. Y.; Nanayakkara, A.; Challacombe, M.; Gill, P. M. W.; Johnson, B.; Chen, W.; Wong, M. W.; Andres, J. L.; Gonzalez, C.; Head-Gordon, M.; Replogle, E. S.; Pople, J. A. *Gaussian 98*, revision A.11.2; Gaussian, Inc.: Pittsburgh, PA, 2001.
(65) Frisch, M. J.; Trucks, G. W.; Schlegel, H. B.; Scuseria, G. E.; Robb, M. A.; Cheeseman, J. R.; Montgomery, J. A., Jr.; Vreven, T.; Kudin, K. N.; Burant, J. C.; Millam, J. M.; Iyengar, S. S.; Tomasi, J.; Barone, V.; Mennucci, B.; Cossi, M.; Scalmani, G.; Rega, N.; Petersson, G. A.; Nakatsuji, H.; Hada, M.; Ehara, M.; Toyota, K.; Fukuda, R.; Hasegawa, J.; Ishida, M.; Nakajima, T.; Honda, Y.; Kitao, O.; Nakai, H.; Klene, M.; Li, X.; Knox, J. E.; Hratchian, H. P.; Cross, J. B.; Bakken, V.; Adamo, C.; Jaramillo, J.; Gomperts, R.; Stratmann, R. E.; Yazyev, O.; Austin, A. J.; Cammi, R.; Pomelli, C.; Ochterski, J. W.; Ayala, P. Y.; Morokuma, K.; Voth, G. A.; Salvador, P.; Dannenberg, J. J.; Zakrzewski, V. G.; Dapprich, S.; Daniels, A. D.; Strain, M. C.; Farkas, O.; Malick, D. K.; Rabuck, A. D.; Raghavachari, K.; Foresman, J. B.; Ortiz, J. V.; Cui, Q.; Baboul, A. G.; Clifford, S.; Cioslowski, J.; Stefanov, B. B.; Liu, G.; Liashenko, A.; Piskorz, P.; Komaromi, I.; Martin, R. L.; Fox, D. J.; Keith, T.; Al-Laham, M. A.; Peng, C. Y.; Nanayakkara, A.; Challacombe, M.; Gill, P. M. W.; Johnson, B.; Chen, W.; Wong, M. W.; Gonzalez, C.; Pople, J. A. *Gaussian 03*, revision D.01; Gaussian, Inc.: Wallingford, CT, 2004.
(66) Frisch, A. E.; Dennington, R. D.; Keith, T. A.; Neilsen, A. B.; Holder, A. J. *GaussView*, revision 3.9; Gaussian, Inc.: Pittsburgh, PA, 2003.
(67) Szori, M.; Fittschen, C.; Csizmadia, I. G.; Viskolcz, B. J. *Chem. Theory Comput.* **2006**, *2*, 1575.
(68) Lipscomb, L. A.; Peek, M. E.; Morningstar, M. L.; Verghis, S. M.; Miller, M.; Rich, A.; Essigmann, J. M.; Williams, L. D. *Proc. Natl. Acad. Sci. U.S.A.* **1995**, *92*, 719.

JP805942Y